

Correlations among notched beam tests, double punch tests and round panel tests for a high performance fibre concrete cast at site

Tan, Kiang Hwee; Walraven, Joost; Grünewald, Steffen; Rovers, John; Cotovanu, Bogdan

DOI

[10.1016/j.cemconcomp.2021.104138](https://doi.org/10.1016/j.cemconcomp.2021.104138)

Publication date

2021

Document Version

Final published version

Published in

Cement and Concrete Composites

Citation (APA)

Tan, K. H., Walraven, J., Grünewald, S., Rovers, J., & Cotovanu, B. (2021). Correlations among notched beam tests, double punch tests and round panel tests for a high performance fibre concrete cast at site. *Cement and Concrete Composites*, 122, Article 104138. <https://doi.org/10.1016/j.cemconcomp.2021.104138>

Important note

To cite this publication, please use the final published version (if applicable). Please check the document version above.

Copyright

Other than for strictly personal use, it is not permitted to download, forward or distribute the text or part of it, without the consent of the author(s) and/or copyright holder(s), unless the work is under an open content license such as Creative Commons.

Takedown policy

Please contact us and provide details if you believe this document breaches copyrights. We will remove access to the work immediately and investigate your claim.



Contents lists available at ScienceDirect

Cement and Concrete Composites

journal homepage: www.elsevier.com/locate/cemconcomp

Correlations among notched beam tests, double punch tests and round panel tests for a high performance fibre concrete cast at site

Kiang Hwee Tan^{a,*}, Joost Walraven^b, Steffen Grünwald^{b,c}, John Rovers^d, Bogdan Cotovanu^d

^a National University of Singapore, Singapore

^b Delft University of Technology, the Netherlands

^c Ghent University, Belgium

^d Shell Global Solutions, Rijswijk, the Netherlands

ARTICLE INFO

Keywords:

High performance
Steel fibre concrete
Test methods
Notched beam test
Double punch test
Round panel test

ABSTRACT

A high performance fibre concrete with a cylinder strength of about 80 MPa was developed and tested both under laboratory and site conditions. The post-cracking properties were determined in a series of three-point notched beam tests according to EN 14651. Subsequently, double punch tests on 150 mm cubes were carried out to verify whether such tests could be used for control of the properties of the concrete cast at site. It was shown that the same relations can be obtained by using simple conversion factors. Additionally, it was studied if it is possible to test round panels according to ASTM C1550-02 to verify the properties of the fibre concrete. Also here, it turned out that it is possible to derive simple conversion factors to relate the results of the round panel tests to those of the notched beam tests. The findings provide useful information for a practical quality assessment with regard to the execution of fibre reinforced concrete structures.

1. Introduction

Fibre reinforced concrete (FRC) is increasingly being used in the construction industry due to the beneficial crack-bridging effect of fibres, thereby enhancing the post-cracking characteristics and the durability of concrete members. Applications of FRC are seen in slab-on-grade and slab-on-pile systems, tunnel segmental linings, and foundation beams, for example, which result in labour saving and increased work productivity.

To ensure the execution control of FRC, tests on notched beam specimens according to EN 14651 are normally required to be carried out on field-prepared specimens to determine the residual flexural tensile strength. The test results however are influenced by the test execution and equipment, and are subject to relatively large variations, and a coefficient of variation of up to 30% could be expected in general. On the other hand, round panel tests according to ASTM C1550-02 may also be carried out to assess the properties of FRC, and this test is known to provide more consistent results. However, due to the larger specimen size, a more complex test set-up and a longer test duration, it is not widely applied as a control test.

The Multilateral Double Punch Test (MDPT) is executed with cube specimens identical to those required for compressive strength tests, to

evaluate the residual tensile properties of FRC. It is a straight-forward test which requires two simple punching wedges without the need for special equipment or test set-up. The test can be completed within several minutes and is subject to relatively less variation in test results. By correlating the test results from both notched beam and double punch tests, it would be possible to carry out the latter in lieu of the former, and this would be very beneficial in a large project where many series of tests need to be carried out as quality assurance.

In 2017/2018, a series of tests has been carried out, aiming at determining the mechanical and physical properties of a specially developed high performance fibre concrete mixture to be used in foundation elements. The reference concrete has an average cube strength of 110 MPa, an axial tensile strength of 4.8 MPa and a post-cracking tensile strength of 6.1 MPa. The concrete contains 60 kg/m³ hooked-end steel fibres and is self-compacting. The suitability of this concrete for practical application was reported in Ref. [1]. It was wondered how such a special concrete, which was developed and tested under laboratory conditions, would behave under site conditions, making use of local materials. Therefore, two new mixtures were developed, based on the same principles but with local materials, which were produced at a construction site on the island of Bukom, Singapore. This occasion was used for casting three series of concrete specimens

* Corresponding author.

E-mail address: tankh@nus.edu.sg (K.H. Tan).

<https://doi.org/10.1016/j.cemconcomp.2021.104138>

Received 18 January 2021; Received in revised form 31 May 2021; Accepted 10 June 2021

Available online 18 June 2021

0958-9465/© 2021 Elsevier Ltd. All rights reserved.

which were subsequently tested.

The program therefore consisted of standard bending tests on notched prisms, double punch tests and round panel tests. As mentioned earlier, the double punch tests were chosen in order to investigate whether those tests could be used as regular control tests for concrete used at the site. The round panel tests were carried out because they are known to generate results with a relatively low scatter, and as such, only a limited number of specimens need be tested.

2. Fibre concrete mixtures used in the investigation

Further to the original laboratory mixtures, used for testing at the Ghent University [1], at the site in Bukom, two alternative mixtures have been produced. Those mixtures have been denoted as “NUS-5” and “NUS-7”. The compositions, and the 28-day cube compressive strengths, are summarized in Table 1.

3. Determination of the post-cracking tensile strength by notched prism tests

Fig. 1a shows a test specimen with a notch, subjected to three-point loading, according to EN 14651. This method of testing is also suggested in the *fib* Model Code 2010 [2]. During the tests, the CMOD (Crack Mouth Opening Displacement) is measured. Fig. 1b shows a typical load – CMOD relation as found in the notched prism test series carried out at the Ghent University (Table 1). This relation can be used to derive the post-cracking strength properties of the fibre concrete. To obtain that, the residual flexural tensile strength f_{Rj} is first calculated for $CMOD_1 = 0.5$ mm and 2.5 mm. This is done with the relation:

$$f_{Rj} = \frac{3F_j l}{2bh_{sp}^2} \quad (1)$$

where: F_j (kN) is the load corresponding to $CMOD = CMOD_j$

l (mm) is the span length

b (mm) is the specimen width

h_{sp} (mm) is the distance between the notch tip and the top of the specimen (125 mm).

From the values, f_{R1} (for $CMOD_1$) and f_{R3} (for $CMOD_3$), the relation between the post-cracking tensile strength and the crack opening is determined as:

$$f_{Ftu} = f_{Fts} - \frac{w_u}{CMOD_3} (f_{Fts} - 0.5f_{R3} + 0.2f_{R1}) \geq 0 \quad (2)$$

where

$$f_{Fts} = 0.45f_{R1} \quad (3)$$

Table 1

Mixture composition (kg/m³) and compressive strength (MPa) of three mixtures.

Constituent	Ghent	NUS 5	NUS 7
Cement	566.5 kg/m ³ (CEM I 52.5)	760 kg/m ³ (CEM III/A 42.5)	748 kg/m ³ (CEM III/A 42.5)
Blast furnace slag	170 kg/m ³	–	–
Silica fume	40 kg/m ³	–	28 kg/m ³
Superplasticizer	6 kg/m ³	11 kg/m ³	10 kg/m ³
Water	192 kg/m ³	201 kg/m ³	199 kg/m ³
Sand	757 kg/m ³	574 kg/m ³	804 kg/m ³
Coarse aggregate	633 kg/m ³ (<6 mm)	816 kg/m ³ (<10 mm)	552 kg/m ³ (<10 mm)
Steel fibres, hooked ends, l/d = 30/0.38 mm/mm	62 kg/m ³	60 kg/m ³	60 kg/m ³
Mean 28-d cube strength (150 × 150 × 150 mm ³)	111 MPa	79.5 MPa	89.4 MPa

and w_u is the maximum crack width accepted in structural design for the failure mode considered. In the *fib* Model Code 2010, $w_u = 1.5$ mm is assumed for failure modes in the ultimate limit state, like shear, torsion and punching. The linear relation according to Eq. (2) is a suitable tool for design purposes. It proceeds from the tensile stress, generated by the fibres directly after cracking, that is, at the onset of crack opening f_{Fts} to the crack opening w_u mentioned before. As such, it is valid for the SLS and ULS stages. For scientific analyses, more advanced expressions are available, for which reference is made to the *fib* Model Code 2010, Chapter 5.6.5 [2].

The mean values $f_{R1,m}$ and $f_{R3,m}$ as found from the tests are listed in Table 2. Any value is a mean result from 12 tests. The characteristic values $f_{R1,k}$ and $f_{R3,k}$ are obtained as the mean value minus 1.71 times the standard deviation.

In the *fib* – MC 2010 also a simplified, rigid-plastic relation is proposed as an alternative for the linear descending branch described by Eq. (2), where after cracking, a constant post-cracking stress is defined at a level $f_{Ftu} = f_{R3}/3$. The application of this relation is limited to the case of design in flexure.

In Ghent, the prisms were cast in the laboratory, whereas in Singapore, the prisms were filled at the building site directly from a truck mixer.

It turns out that the coefficients of variation are relatively small, whereas for traditional fibre concrete, for bending tests on notched prisms, a much higher variation is expected, with COV's generally above 20% [3,4].

The values given in Table 2 are used to derive the post-cracking stress – crack width relation, according to Eqs. (2) and (3). The most important post-cracking tensile strength parameters, determined in this way, are shown in Table 3.

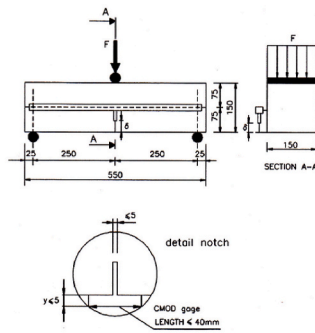
The corresponding post-cracking stress – crack opening relations for the three mixtures, found in this way, are shown in Fig. 2. It is seen that the differences in behaviour among the mixtures in the post-cracking stage are not large. The differences in the compressive strength (Table 1, last line) have only a limited influence on the post-cracking behaviour.

3. Determination of post-cracking behaviour by multilateral double punch test (MDBT)

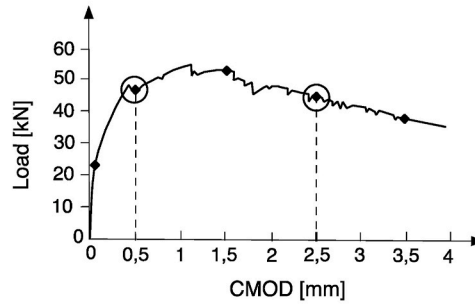
As mentioned earlier, the testing method with notched prisms is generally accepted as a basis for recommendations, but has the disadvantage of a relatively large scatter, so that many tests are necessary. Furthermore, this method is not very practical for verification of the properties for control purposes at the construction site.

A possible alternative for site-control could be the double punch tests (or the “Barcelona test”, see Molins et al. [4], Galeote et al. [5] and Pujadas et al. [6]). For this test, often cylindrical specimens are used, which are loaded at top and bottom through a round steel plate with defined dimensions. Fig. 3a shows the principle of the test in combination with the expected failure mode, which is normally characterized by three radial cracks (Fig. 3b). The parts between the cracks are pushed apart by a wedge-shaped cone of concrete, which forms below the circular steel plates, through which the axial load is introduced. The height of the specimen is mostly 150 mm; the specimens are obtained by halving a 300 mm high cylindrical cast sample. The test is carried out to determine the relation between the vertical force and the “total circumferential opening displacement” (TCOD). The TCOD is predominantly the result of widening of the radial cracks, due to the effect of the push-in, measured by a circumferential extensometer, placed at mid-height around the specimen. Advantages of such a test in comparison with the bending tests on notched prisms are the lower weight, easier testing procedure with time savings and a reduced scatter.

A comparison with results of four-point bending tests showed that it is possible to find a correlation on the basis of energy absorption [4,5].



a. Bending test on notched prism



b. Load – CMOD relations for Prism 1 in Ghent series

Fig. 1. (a) Bending test on notched prism. (b). Load – CMOD relations for Prism 1 in Ghent series.

Table 2

Measured mean values of $f_{R1,m}$ and $f_{R3,m}$ with the corresponding coefficients of variation (CoV) for the three tests series on notched beams subjected to three point loading.

Ghent University	$f_{R1,m} = 13.6$ MPa	CoV = 11.6%	$f_{R1,k} = 10.9$ MPa
	$f_{R3,m} = 11.2$ MPa	CoV = 14.3%	$f_{R3,k} = 8.3$ MPa
NUS-5	$f_{R1,m} = 10.6$ MPa	CoV = 11.3%	$f_{R1,k} = 8.5$ MPa
	$f_{R3,m} = 11.0$ MPa	CoV = 12.7%	$f_{R3,k} = 8.6$ MPa
NUS-7	$f_{R1,m} = 12.9$ MPa	CoV = 16.3%	$f_{R1,k} = 9.4$ MPa
	$f_{R3,m} = 11.9$ MPa	CoV = 21.0%	$f_{R3,k} = 7.7$ MPa

Table 3

Tensile strength values in the post-cracking stage relevant for design.

Symbol	Denotation	Values (MPa) for			Significance for design
		Ghent	NUS-5	NUS-7	
$f_{Ft,m}$	Mean axial tensile strength (post-cracking) at ULS ($w_u = 1.5$ mm)	4.1	3.9	4.3	Analysis of behaviour in ULS
$f_{Ft,k}$	Characteristic tensile strength (post-cracking) at ULS ($w_u = 1.5$ mm)	3.1	3.1	2.8	Determination of bearing resistance in ULS (bending, shear, punching, torsion)
$f_{Ft,m}$	Mean axial tensile stress (post-cracking) at small crack width (SLS)	6.1	4.8	5.8	Crack width control
$f_{Ft,k}$	Characteristic axial tensile stress (post-cracking) at small crack width (SLS)	4.9	3.8	4.2	Tensile stress verification for hardening FRC according to fib MC 2010
$f_{ct,m}$	Mean value of tensile strength at first cracking	4.8	4.6	4.3	Crack width control

An alternative double punch test method (the “Multiple Double Punch (MDP) Test”) was introduced [6]. Instead of cylindrical specimens, it was proposed to use cubic specimens ($150 \times 150 \times 150$ mm³) for double punch tests. This offers the possibility to study the effect of fibre orientation, because a cube can be tested in the three principal directions. Moreover, the TCOD is not measured anymore: the tests are controlled by measuring only the axial force and the axial displacement of the upper loading plate. Three stages of behaviour are distinguished as shown by Fig. 4.

Stage 1 coincides with the initial application of the load. The radial internal stress generated is resisted by the concrete matrix that prevents major cracks. Once the stress reaches the tensile strength of the concrete, the specimen enters Stage 2. The upper and the lower concrete wedges

below the load-introducing steel plates are abruptly formed. These wedges have a conical shape with a diameter equal to that of the round steel plates used in the test. Between two to four radial cracks appear, dividing the specimen in parts that are kept together by the fibres bridging the cracks. As the cracks stabilize, Stage 3 starts, following a kinematic mechanism that involves sliding between the conical wedge and the fragmented specimen, as illustrated in Fig. 4.

For each of the mixtures NUS-5 and NUS-7, 24 MDP-tests were carried out. Twelve of those tests were carried out with the load in the direction of casting (Z-direction, Fig. 5). The other 12 tests were carried out in the direction perpendicular to the casting direction (X-Y direction), Fig. 5.

Fig. 6 shows the load – axial displacement relations for mixture NUS-5. In Fig. 6a, the results are shown for specimens loaded in the X- or Y-direction (perpendicular to the casting direction) whereas Fig. 6b shows the results where the load was applied in the Z-direction (casting direction).

It turns out that in both cases the scatter of the results is small. Moreover, it is seen that the resistance of the specimens in the post-cracking stage is larger if they are tested in the direction of casting (Z-direction). This is most probably caused by fibre orientation. The cube formwork has been filled at the production site from a truck mixer through a half pipe, where the fibres may have oriented before entering in the formwork. Loading of the hardened cubes in casting direction leads to a situation where the formation and widening of vertical cracks is effectively counteracted by the fibres with a horizontal orientation, which influences the reaction of the specimens and the strength properties.

During testing, typically two radial cracks were observed in each specimen, see Fig. 7.

A question is whether the results of those tests can be correlated with the results of the notched prism tests. Here, not the energy absorption has been used as a basis for correlation [4–6] but a simple empirical relation has been derived. To this aim, it is assumed that the post-cracking tensile stress σ_{Ft} in the radial cracks is proportional to the axial load P on the specimen, in any stage of the deformation, so:

$$\sigma_{Ft} = c_1 \cdot P \tag{4}$$

with σ_{Ft} in (MPa) and P in (kN). Furthermore, it is assumed that there is a linear relation between the width of the radial cracks w and the post-peak axial shortening δ , so:

$$w = c_2 \cdot \delta \tag{5}$$

where w and δ are in (mm).

Here, δ is the net axial displacement, defined as the total axial displacement minus the axial displacement at peak load.

The values of c_1 and c_2 can be determined by comparing the $P - \delta$ relations found in the MDP-tests and the linear relations found by the

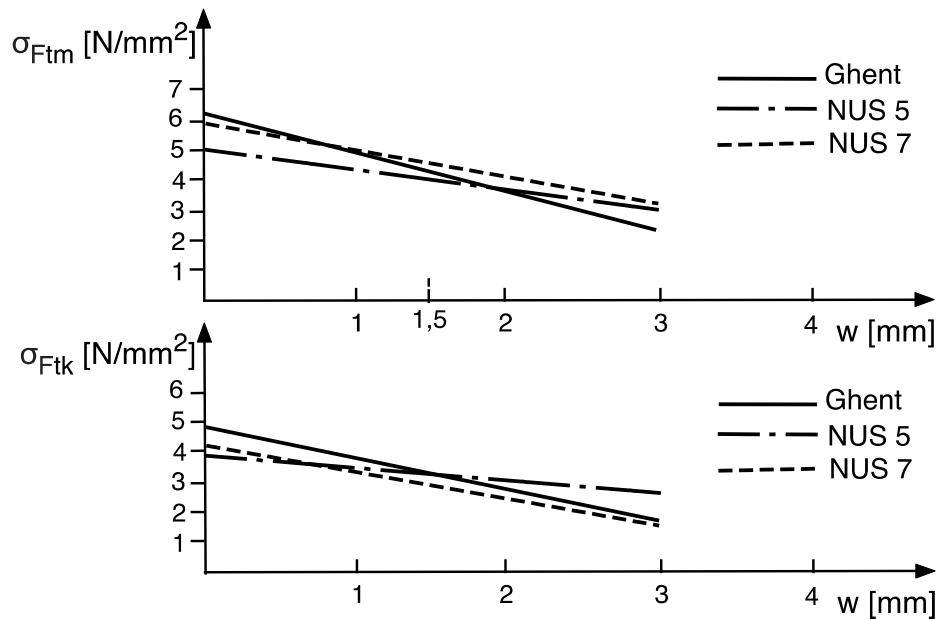


Fig. 2. Relation between post-cracking tensile stresses σ_{Ftm} and σ_{Ftk} and crack opening w , for the three mixtures considered (Tables 2 and 3), according to Eq. (2).

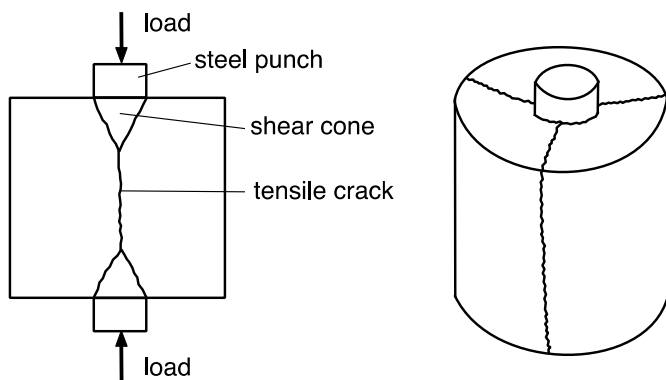


Fig. 3. Principle of the Double Punch Test [4]: a. Geometry of the Double Punch Test specimen; b. Formation of three radial cracks due to wedging action below the load introduction plate.

notched-prism tests.

It turns out that for $c_1 = 0.023$ and $c_2 = 1.0$ for the MDP specimens loaded in the casting (Z-) direction, good agreement is found between the two test methods. This is shown in Fig. 8, where the descending $\sigma - w$ lines for the mixtures NUS-5 and NUS-7, obtained from bending tests on

notched prisms, given in Fig. 2 (upper figure) are compared with the experimental results obtained from the MDP-tests. In this figure, the horizontal axes for crack width and displacement have the same scale, so $c_2 = 1$. On the other hand, the vertical axes for post-cracking tensile stress f_{Pt} and axial load P have different scales, in the ratio of 2.3 MPa–100 kN, which corresponds with $c_1 = 0.023$. In this way, a direct comparison is possible.

This shows that the MDP-tests could be used as an alternative to the three-point bending test (with notched beams) to obtain the stress-crack opening constitutive law, provided that the test specimen is loaded in the direction of concrete casting. The MDP tests are also suitable for the control of the concrete properties at the site.

5. Determination of post-cracking behaviour by round panel test

5.1. Experiments

Further to the bending tests on notched prisms and the multiple double punch tests, treated previously, tests have been carried out on round panels. For both mixtures NUS-5 and NUS-7, a series of four tests was carried out. The tests were carried out according to ASTM C1550-02 [7]. According to those recommendations, the panels have a radius $R = 400$ mm and a thickness, h , equal to 75 mm. The panels are supported at three points near to the perimeter of the slab as shown in Fig. 9. A point

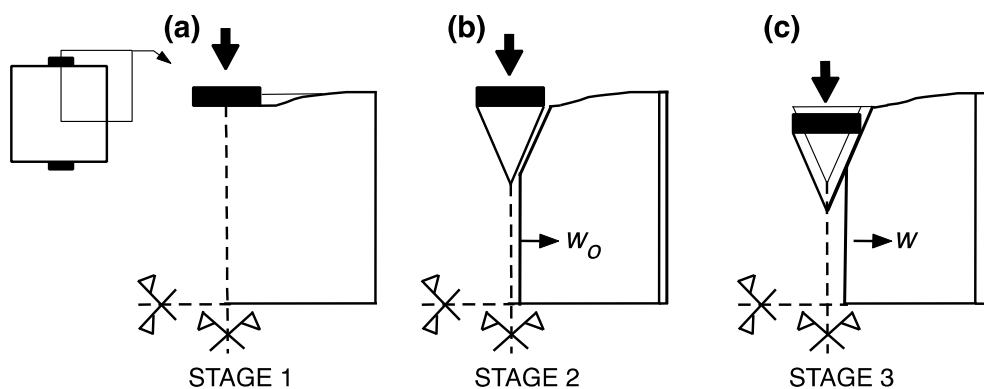


Fig. 4. Stages 1–3 of multiple double punch tests executed on a cube.

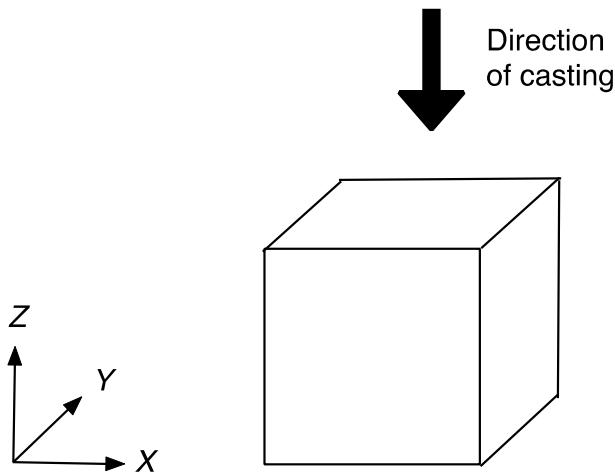


Fig. 5. Directions of loading versus casting direction.

load is applied in the centre of the round panel. During loading mostly three radial cracks occurred at angles of about 120° .

The measured dimensions of the slab and the peak loads are given in Tables 4a and 4b. Because the thickness of the slabs deviated slightly from 75 mm, the measured peak values of the loads have been corrected according to ASTM C1550. In Tables 4a and 4b both the measured and the corrected values are given.

The measured load-displacement relations are shown in Fig. 10a and b. The series NUS-5 shows more scatter in the peak load (which largely disappears after correction) but less scatter in the post-peak behaviour, which reduces with increasing crack width. The COV for the peak loads

observed in the round panel tests series is substantially lower than for the notched prism tests.

The crack patterns observed for the series tests on panels with mixture NUS-5 are shown in Fig. 11.

5.2. Analysis of results with rigid plastic post-cracking stress – crack opening relation

For the interpretation of round panel tests, several models have been proposed [8–12]. Most of the evaluations concentrate on classical fibre concrete, with softening behaviour after cracking. The fibre concrete considered in the actual investigation, however, is a high performance concrete with a hardening behaviour after cracking, with $f_{Fstm} > f_{ctm}$ (see Table 3). This effect will be taken into consideration in the present paper.

The fib Model Code of Concrete Structures 2010 [2] considers two ways of describing the development of the tensile stress after cracking [2]. The simplest method is the “rigid-plastic” approach (constant tensile stress $f_{Ftu} = f_{R3}/3$ at crack widening). The more advanced formulation deals with a linearly decreasing value of f_{Ftu} after cracking, with increasing crack width, see Eq.(2). As a first approach, the relation between peak load and the post-cracking strength f_{Ftu} is investigated assuming rigid-plastic behaviour.

For the analysis of the results, it is assumed that the behaviour can be simplified to that of a panel with three radial cracks at angles of 120° . Those cracks work as yield lines as a result of the effect of the steel fibres. The uncracked segments between the yield lines are assumed to be rigid, see Fig. 12

Based on the yield line moment capacity m_y (per unit length of the crack), the central point load capacity P can be calculated as:

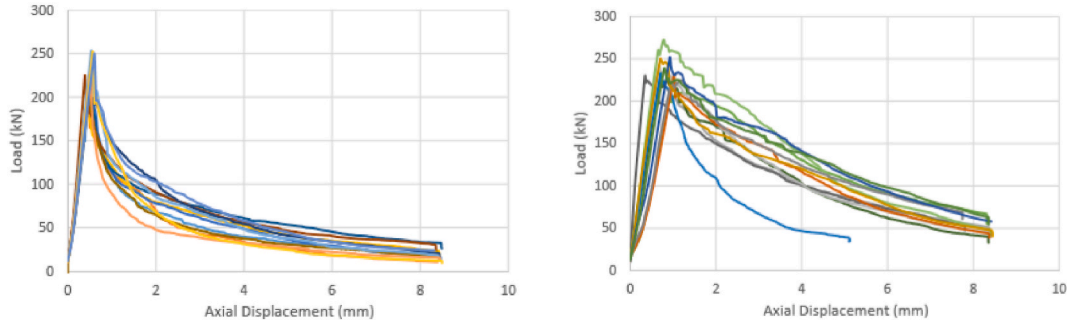


Fig. 6. Load – axial displacement relations for MDP-tests carried out on mixture NUS-5. a) tests with loading in X- or Y-direction (perpendicular to the casting direction) b) tests with loading in the Z-direction (in the casting direction).

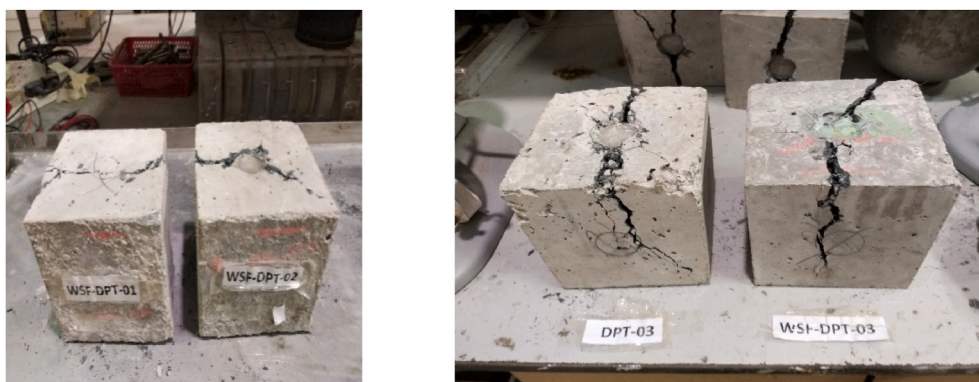


Fig. 7. Radial cracking in MDP-test (mixture NUS-7).

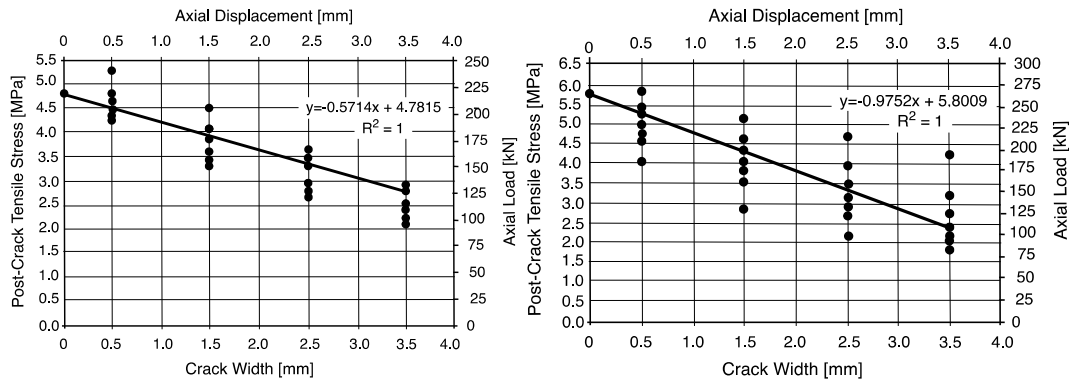


Fig. 8. Comparison between stress – crack opening relations as determined by tests on notched beams (descending lines) and results obtained with double punch tests (spots) for the two different mixtures NUS-5 and NUS-7.

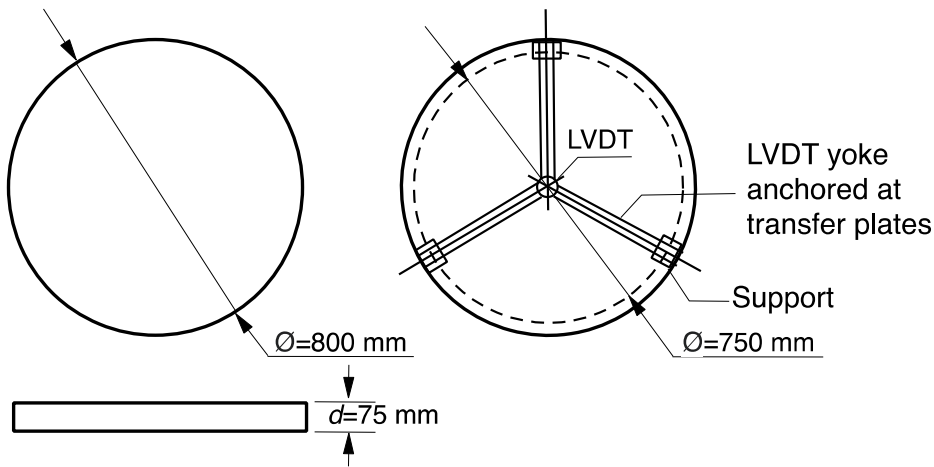


Fig. 9. Test method on round panels according to ASTM C1550.

Table 4a
Results of Round Panel tests for mixture NUS-5.

	Thickness <i>h</i> (mm)	Diameter <i>d</i> (mm)	Measured peak load <i>P</i> (kN)	Corrected peak load <i>P</i> (kN)	No. of radial cracks	Remarks
NUS5-01	78.5	800	55.8	50.9	3	
NUS5-02	81.5	800	65.1	55.1	3	
NUS5-03	80.9	800	60.5	52.0	3	1 other minor crack
NUS5-04	83.4	800	70.3	56.9	3	
			$P_{meas,m} = 62.9$	$P_{corr,m} = 53.7$ cov = 5.1%		

Table 4b
Results of Round Panel tests for mixture NUS-7.

	Thickness <i>h</i> (mm)	Diameter <i>d</i> (mm)	Measured peak load <i>P</i> (kN)	Corrected peak load <i>P</i> (kN)	No. of radial cracks	Remarks
NUS7-01	83.0	800	81.6	66.7	3	2 other minor cracks
NUS7-02	78.4	800	73.0	66.8	3	
NUS7-03	81.6	800	78.2	66.1	3	
NUS7-04	80.8	800	81.8	70.4	3	1 other minor crack
			$P_{meas,m} = 78.7$	$P_{corr,m} = 67.5$ cov = 2.9%		

$$P = \frac{3 \cdot m_y \cdot \cos 30^\circ \cdot 2 \cdot R}{r} \tag{6}$$

where m_y is the yielding (plastic) moment, R is the radius of the panel and r is the distance between the centre of the slab and the centre of the supports ($R = 400$ mm and $r = 375$ mm).

The relation between the central deflection δ and the crack opening w , which is assumed constant along the crack, is equal to:

$$\delta = \frac{w \cdot r}{2 \cdot \cos 30^\circ (h - x)} \tag{7}$$

where x is the height of the compression zone.

The yielding (“plastic”) moment can be expressed as:

$$m_y = 0.5 f_{tu} h^2 \text{ (per unit width)} \tag{8}$$

This expression is based on the assumption of a constant post-

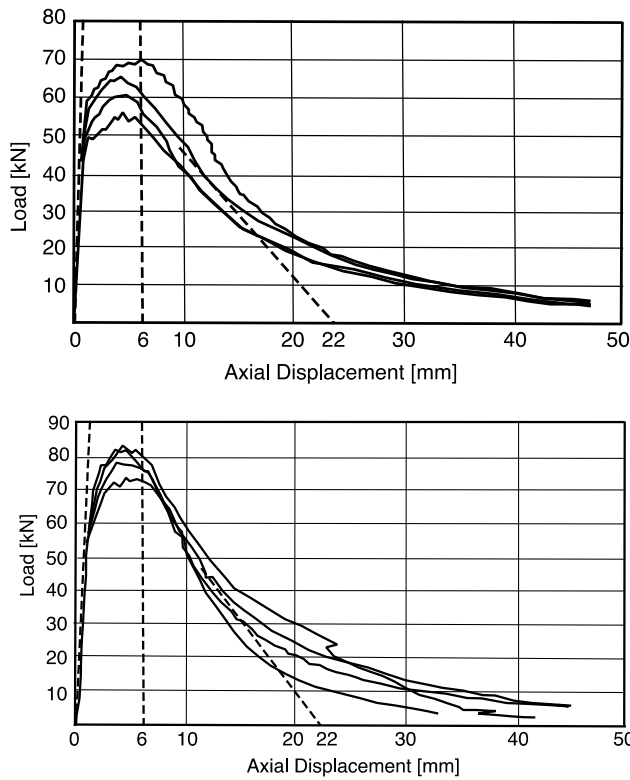


Fig. 10. Measured load-deflection relations for two series of round panel tests (see Tables 4a and 4b): (a) for mixture NUS-5, upper diagram, (b) for mixture NUS-7, lower diagram.

cracking tensile stress f_{Ftu} in the tensile zone of the cross-section, see Fig. 13. As mentioned in Section 3, the rigid-plastic relation is suitable for the case of bending.

Inserting Eq. (8) in Eq. (6) leads to the following relation between the maximum load on the slab and the post-cracking tensile strength f_{Ftu} :

$$f_{Ftu} = \frac{r}{3h^2R\cos 30^\circ} \cdot P_{max} \tag{9}$$

Four panel tests were carried out on concrete mixture NUS-5. The mean value of P_{max} was reported to be 53.7 kN (after correction). Inserting this into Eq. (9) results in a value $f_{Ftu} = 3.44$ MPa. With the same concrete, a series of tests on notched beams was carried out, as already described in Section 2 of this paper. The corresponding value for f_{Ftu} following from those tests was $f_{Ftu} = 3.9$ MPa, so the agreement with the result of the round panel test was reasonable (difference 12%). In the second series with concrete type NUS-7, a mean value for $P_{max} = 67.5$ kN was reported. With Eq. (9), this leads to a value $f_{Ftu} = 4.3$ MPa. With the earlier series of notched beam tests, a value $f_{Ftu} = 4.3$ MPa was obtained. In this case, the agreement is perfect.

5.3. Determination of linearly descending stress-crack width relation

In order to analyse the test results in a different way, it is assumed that the relation between post-cracking strength and crack width follows the relation shown in Fig. 14.

Considering the load-deflection relations in Fig. 10, three stages of behaviour can be distinguished:

- A linear ascending $P-\delta$ branch, which starts to deviate from linearity at first cracking;
- A crack formation stage, where the load-displacement curve is characterized by a type of inverse parabolic shape. In this stage, the specimen develops from an uncracked element with linear elastic

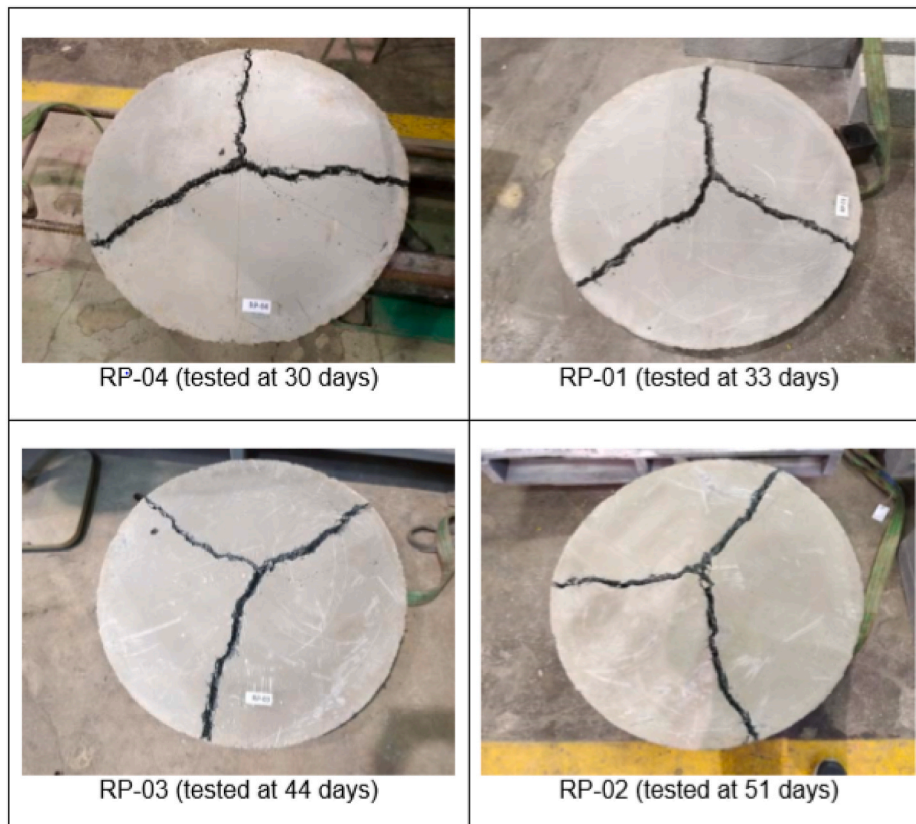


Fig. 11. Crack patterns of the four panels tested in series NUS-5.

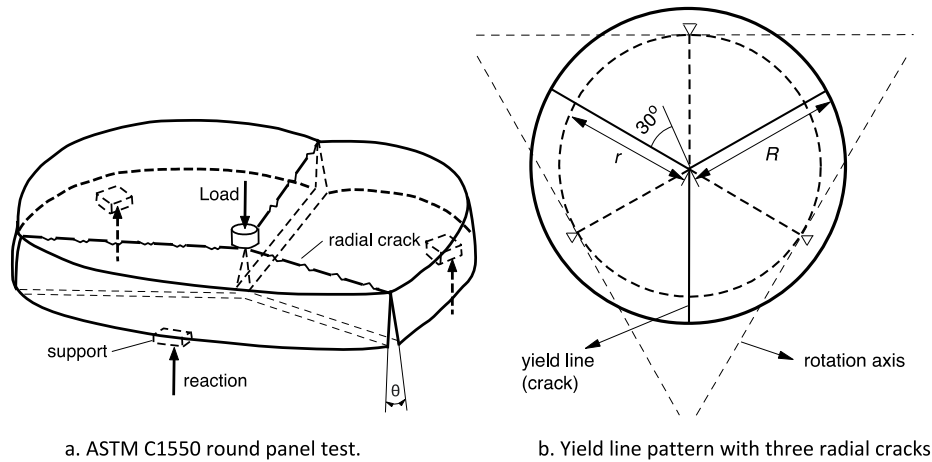


Fig. 12. (a) ASTM C1550 round panel test. (b). Yield line pattern with three radial cracks.

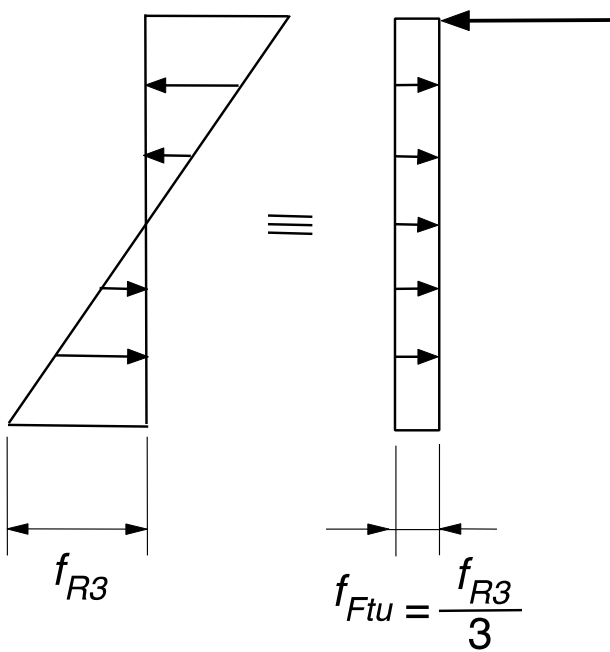


Fig. 13. Simplified model for the yielding moment [2].

behaviour to a slab mechanism with three yield lines (testified by three radial cracks at angles of about 120° with each other, with quasi-rigid segments in between);

- A linear descending branch, starting from the end of the crack formation stage, in agreement with the expected behaviour of the yield line model, with stiff segments in between the radial cracks.

The existence of a crack formation stage, shown in Fig. 10 for the NUS panel tests, can be explained on the basis of the hardening behaviour of the concrete used to produce the specimens: the post-cracking tensile strength f_{Ftsm} of this concrete is higher than the first-cracking strength f_{ctm} , which leads to multiple crack formation. Only after further deformation (axial displacement), those bundles of fine cracks develop into discrete cracks, which start to act as yield lines.

The linear descending relation, corresponding with the yield line model, starts at an axial displacement of about 6 mm (end of crack formation stage) see Fig. 10a and b. Since the elastic deformation at the start of the crack formation stage is about 1 mm, the central deflection during crack formation is about $\delta = 5$ mm. According to Eq. (7) this corresponds with a crack width of about $0.312 \cdot 5 = 1.56$ mm (assuming $x = 0.1h$). So, when the yield line mechanism starts to get active at about $\delta = 6$ mm, there is already an initial crack opening that should be taken into account in the analysis.

The descending linearized $P - \delta$ relation initially covers the experimental curves quite well, but starts to deviate after the load has been reduced to about 40% of the top value (Fig. 10a and b). This might partially be caused by some curvature in the uncracked portions of the panel between the radial cracks (which are not perfectly rigid). Also

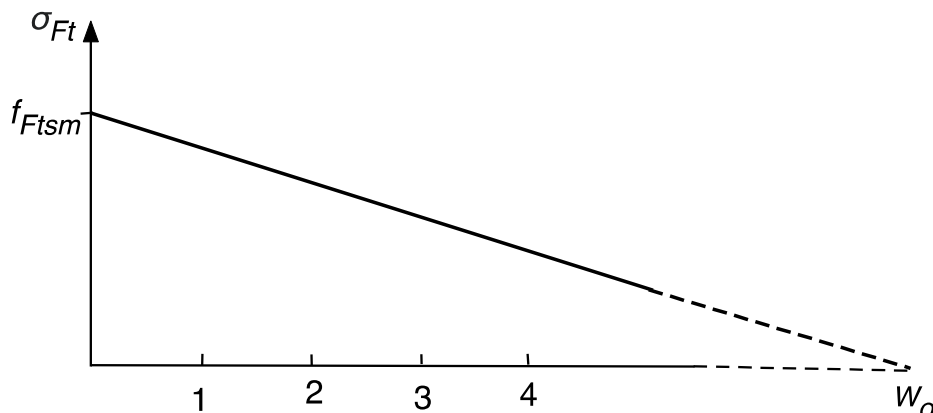


Fig. 14. Assumed relation between post-cracking tensile stress σ_{Ft} and crack width w according to fib MC 2010.

membrane effects at larger deflections can lead to a non-uniform distribution of crack width along each radial crack. Moreover, the beginning of fibre pull-out could play a role.

It should, however, be realized that this nonlinear behaviour occurs at axial displacements (and corresponding crack widths) which are out of the range of practical situations: a central deflection of $\delta = 20$ mm corresponds with a width of the radial cracks of about 6 mm, where in codes for fibre concrete, like [2], in design calculations, crack widths of 1.5–2.5 mm are regarded as maximum allowable values in the ULS. Therefore, in the analysis, the nonlinear part of the descending relation is outside the area of practical relevance and is therefore not taken into account. For the analysis, it is assumed that the linear descending branch is followed until the horizontal axis is reached. This intersection point δ_0 (22 mm at the horizontal axis in Fig. 10a and b) can be related to the value of w_0 shown in Fig. 14, enabling a comparison with the $\sigma - w$ relations derived from the series of notched beam tests.

In Section 6.2, a number of equations have been given which will be used in the analysis. Eq. (6) gives the relation between the force P acting on the structure and the yield line moment m_y (per unit width of the yield line). Eq. (7) gives the relation between the central deflection δ and the crack width w , also conforming the yield line mechanism. Eq. (8) gives an expression for the yield line moment m_y , based on a simplified assumption for the forces in the cross-section (compression force in top of cross section, Fig. 13). In the following analysis, a cross-section with a compression zone of $x = 0.1h$ will be assumed.

Inserting $R = 400$ mm and $r = 375$ mm into Eq. (6) results in:

$$P = 5.54m_y \tag{10}$$

Inserting $r = 375$ mm, $h = 75$ mm and $x = 0.1h$ into Eq. (7) leads to:

$$\delta = 3.2w \text{ or} \tag{11a}$$

$$w = 0.31\delta \tag{11b}$$

For the derivation of the yielding moment acting in the yield lines, it is assumed that there is a compressive zone with a depth of $0.1h$. Furthermore, it is assumed that the distribution of the post-cracking tensile stress over the tensile zone is influenced by the effect of pre-cracking, before the yield line mechanism starts to be active. At the onset of further crack opening according to the yield line model (start of linear part of the descending load – deflection relation), the stress distribution is assumed to be as shown in Fig. 15.

The stress distribution in the tensile zone runs from a value f_{Ftsm} at the top of the cracked concrete zone, to a reduced value $f_{Ftsm} - \Delta f_{Ft}$. At the start of the activation of the yield line model, the stress-reduction Δf_{Ft} is due to the initial crack width developed in the crack formation stage, which is equal to $w_x = 0.31\delta = 0.31 \cdot 5 = 1.56$ mm (as mentioned previously). The relation between crack width and stress increment Δf_{Ft} follows from the relation shown in Fig. 15, right. This relation is:

$$\frac{\Delta f_{Ft}}{f_{Ftsm}} = \frac{w_x}{w_0} \tag{12}$$

With $w_x = 1.56$ mm, this leads to:

$$\Delta f_{Ft} = \frac{1.56}{w_0} f_{Ftsm} \tag{13}$$

The yield moment per unit width can now be calculated as:

$$m_y = (0.9h \cdot f_{Ftsm}) \cdot 0.5h - \left\{ 0.5 \left(\frac{1.56}{w_0} \cdot f_{Ftsm} \right) \cdot 0.9h \right\} \cdot 0.65h \tag{14}$$

which can be simplified to:

$$m_y = f_{Ftsm} \cdot 0.45h^2 \left(1 - \frac{1}{w_0} \right) \tag{15}$$

The relation between the load P_{max} on the structure and the yield moment m_y follows from Eq. (10), so:

$$P_{max} = 5.54f_{Ftsm} \cdot 0.45h^2 \left(1 - \frac{1}{w_0} \right) \tag{16}$$

So the value of f_{Ftsm} can immediately be expressed as a function of P_{max} and w_0 on basis of Eq. (16). After inserting $h = 75$ mm in this equation it is found that:

$$f_{Ftsm} = 7.13 \cdot 10^{-5} \frac{P_{max}}{\left(1 - \frac{1}{w_0} \right)} \tag{17}$$

The values P_{max} (in N) and w_0 (in mm) follow directly from the round panel tests. Under axial tension, w_0 is the crack width at which no tensile stresses are transmitted anymore across a crack in fibre reinforced concrete. As a practical assumption, w_0 has been adopted to be a function of the value δ_0 which is the intersection point between the dotted line representing the mean linear descending relation, and the horizontal axis, see Fig. 10a and b.

As listed in Table 4a, the series of four tests on panels of mixture NUS-5 gave a mean peak load $P_{max} = 53700$ N. For the intersection point a value $\delta_0 = 22$ mm is found (Fig. 10a). According to Eq. (11b), this corresponds to $w_0 = 0.31 \cdot 22 = 6.82$ mm. Inserting the values for P_{max} and w_0 in Eq. (17), it is found that $f_{Ftsm} = 4.5$ MPa.

With the values $f_{Ftsm} = 4.5$ MPa and $w_0 = 6.82$ mm the relation between post-cracking tensile stress σ_t and the crack width w is defined. In Fig. 16a, this relation is compared with the relation derived earlier for the same fibre concrete mixture from a series of notched beam tests, see Fig. 2, upper diagram, which is the line for NUS-5. The agreement is good.

The same approach can be followed for the other series of panel tests with concrete NUS-7. In Table 4b, a corrected peak load of $P_{max} = 67500$

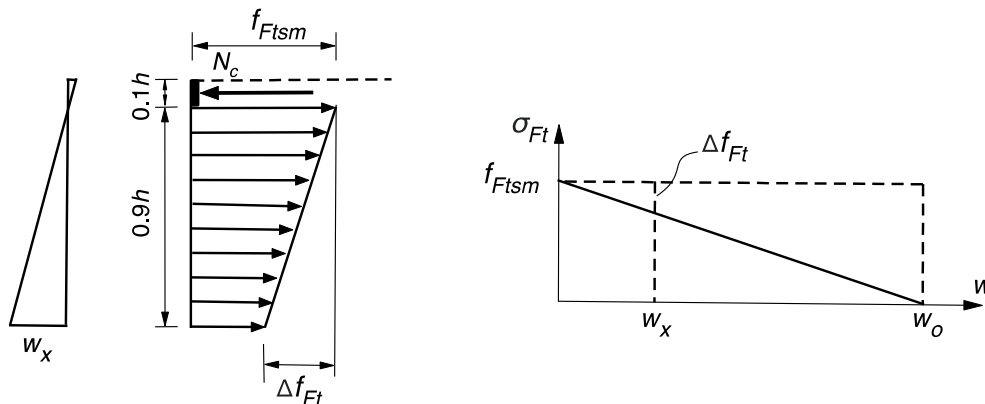


Fig. 15. Determination of stress distribution in cross-section.

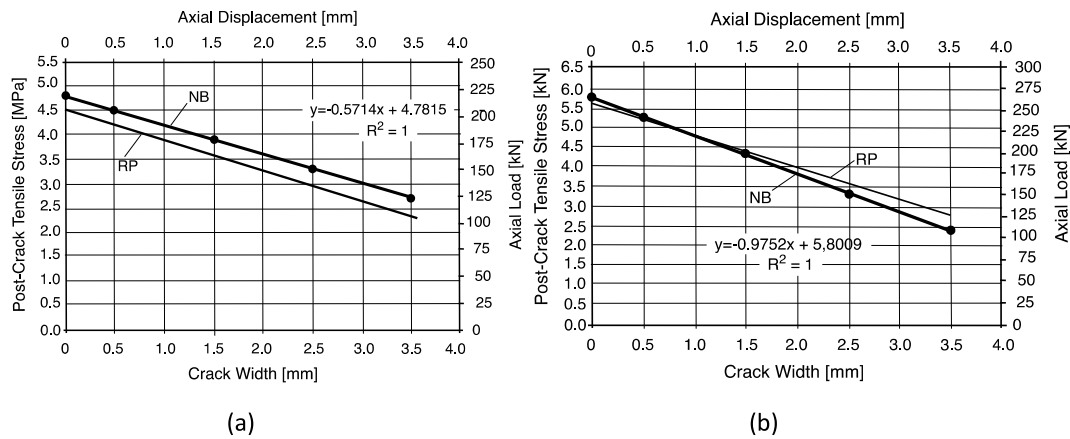


Fig. 16. Post-cracking tensile stress – crack width relations derived from notched beam tests (NB-lines) and from the round panel tests (RP-lines): a) for mixture NUS-5; b) for mixture NUS-7.

N was reported. Also, for this series an intersection point $\delta_0 = 22$ mm was found, so that also here, $w_0 = 6.82$ mm. Inserting those values in Eq. (17) gives $f_{Ftsm} = 5.64$ MPa. In Fig. 16b, the $\sigma_{Ft} - w$ relation obtained from the round panel tests is compared with the relation derived earlier from the notched beam tests for the same mixture at NUS, see Fig. 2, upper diagram, line for NUS-7. The agreement is very good.

5.4. Conclusions for the round panel tests

1. The stress–crack width relations derived from round panel tests, based on the assumption of a yield line mechanism and taking account of the effect of a crack formation stage due to hardening of the concrete in tension, correspond very well with the relations determined earlier on the basis of a series of notched beam tests;
2. The derivation of a stress–crack opening relation from the results of a round panel test is relatively easy. The relation can immediately be derived from the maximum load P_{max} and the intersection point δ_0 between the linear part of the descending branch and the horizontal axis of the $P-\delta$ relation. Those values follow directly from the load – displacement relations observed in the test;
3. The behaviour of a round panel made of a hardening fibre concrete, as used in the tests described here, differs from the generally observed behaviour in case of standard (softening) fibre concrete applications. For the evaluation of round panel tests with a hardening behaviour due account should be taken of the crack formation stage, where multiple cracks concentrate to become single radial cracks;
4. The relations obtained by round panel tests have a substantially lower coefficient of variation than the relations obtained from the notched beam tests; so the method is adequate and valuable as an alternative test method, or for control of the fibre concrete tensile properties at the construction site. In such a case a comparison of the mean values of the results obtained from notched prisms tests and round panel tests should be appropriate.

6. General conclusions

The findings of the study are highlighted as follows:

1. A self-compacting high performance fibre concrete, which was developed at the University of Ghent was reproduced at a construction site at Bukom (Singapore, temperature at casting 37 °C) under considerably less favourable conditions than in the laboratory. The 28-day concrete compressive strength achieved at the site was about 25% lower than obtained under laboratory conditions in Ghent. The difference can be explained by the use of local materials,

in particular the higher water demand of the aggregates and the lower norm strength of the available cement. However, the behaviour in the post-cracking stage is obviously less sensitive to the local conditions.

2. The tensile stresses of the fibre concrete mixtures made at the site were, in the post-cracking stage, slightly lower than the values from the tests carried out under laboratory conditions. For the design values, derived from the bending tests on notched prisms, the differences were surprisingly small.
3. The results of the double punch tests conducted at NUS, showed a very good agreement with the values obtained by the notched beam tests in the same laboratory. It was shown that only very simple relations between, on the one hand, the axial tensile load and tensile stress in cracked fibre concrete, and on the other hand between the axial shortening and the crack width, are sufficient to obtain nearly similar stress – crack opening relations as determined with the standard tests on notched prisms. Therefore, the double punch test is suitable to be used for control of properties of the fibre concrete at the building site. This control should be carried out for the mean values of the post-cracking tensile strength results.
4. The round panel tests show a very small variation in the results. This is favourable, in the sense that a small number of tests leads already to a reliable prediction of the mean value of the material parameters. The coefficient of variation in a series of round panel tests is small, because of the relatively large area of the crack faces oriented in different directions, so that local inconsistencies in fibre orientation are compensated by the redistribution capacity of the panel. This could also mean that the variability of the results of round panel testing underestimate the variability in material properties in a FRC structure cast at site. In this respect, however, it should be realized that for any test method, the variability of test results is not fully representative for the variability of the properties in a structure. A design recommendation for fibre concrete should therefore always take account of, on the one hand, the possibility of local deviations in fibre orientation and, on the other hand, the redistribution capacity of the structure in compensating local inconsistencies due to local non-uniform fibre orientation.
5. Although the round panel test is favourable in terms of small scatter in test results, it requires much more work in preparation and testing of specimens, and therefore may not be practical. The double punch test, however, promises to be a good substitute for notched beam tests in large-scale projects in particular once it has been calibrated, as it is simpler and easier to carry out, as demonstrated for the self-compacting high-performance concrete in this study.

Declaration of competing interest

The authors declare that they have no known competing financial interests or personal relationships that could have appeared to influence the work reported in this paper.

References

- [1] D. Droogné, L. Taerwe, J. Walraven, B. Cotovanu, Tests on the application of high strength self-compacting reinforced concrete in foundation elements, in: *Fib Symposium Cracow 2019, Proceedings*, 2019, pp. 235–424.
- [2] fib (Fédération Internationale du Béton), Model Code for Concrete Structures 2010, 2010.
- [3] B. Parmentier, E. De Grove, L. Vandewalle, F. Van Rickstal, Dispersion of the mechanical properties of FRC investigated by different ending tests, in: *Proceedings of the Fib Symposium "Tailor Made Concrete Structures*, Taylor & Francis Group, Amsterdam, 2008, pp. 507–512.
- [4] C. Molins, A. Aguado, S. Saludes, Double punch test to control the energy dissipation in tension of FRC (Barcelona test), *Mater. Struct.* 42 (4) (2009) 415–425.
- [5] E. Galeote, A. Blanco, S. Cavalaro, A. de la Fuente, Correlation between the Barcelona test and the bending test in fibre reinforced concrete, *Construct. Build. Mater.* 152 (2017) 529–538.
- [6] P. Pujadas, A. Blanco, S. Cavalaro, A. de la Fuente, A. Aguado, Multidirectional double punch test to assess the post-cracking behaviour and fibre orientation of FRC, *Construct. Build. Mater.* 58 (2014) 214–224.
- [7] Astm International Standard C1550-02, Standard Test Method for Flexural Toughness of Fibre Reinforced Concrete (Using Centrally Loaded Round Panel), 2002. Edition Sept. 2002.
- [8] F. Minelli, G. Plizarri, Fibre reinforced concrete characterization through round panel test – Part I: experimental study, in: *Fracture Mechanics of Concrete and Concrete Structures, Korea 2010, Proceedings*, 2010, pp. 1451–1460.
- [9] F. Minelli, G. Plizarri, Fibre reinforced concrete characterization through round panel test – Part II: analytical and numerical study, in: *Fracture Mechanics of Concrete and Concrete Structures, Korea, 2010, Proceedings*, 2010, pp. 1461–1468.
- [10] F. Minelli, G. Plizarri, A new round panel test for the characterization of fibre reinforced concrete: a broad experimental study, *J. Test. Eval.* 39 (5) (2011).
- [11] F. Minelli, G. Plizarri, Derivation of a simplified stress-crack width law for Fibre Reinforced Concrete through a revised round panel test, *Cement Concr. Compos.* 58 (2015) 95–104.
- [12] L. Vandewalle, F. van Rickstal, B. Heirman, B. Parmentier, On the round panel and 3-point bending tests, in: *BEFIB 2008, 7th RILEM International Symposium on Fibre Reinforced Concrete, Proceedings*, 2008, pp. 173–182.